AGU PUBLICATIONS

Geochemistry, Geophysics, Geosystems

RESEARCH ARTICLE
10.1002/2017GC007014

Key Points:
- Ratios of geodetic to geologic rates prior to large earthquakes are diverse
- Observations show fault-system behavior is not yet fully explained by extant models
- Multiple intrinsic and extrinsic processes may interact to control fault behavior

Correspondence to:
J. F. Dolan,
dolan@usc.edu

Citation:
Dolan, J. F., & Meade, B. J. (2017). A comparison of geodetic and geologic rates prior to large strike-slip earthquakes: A diversity of earthquake-cycle behaviors? *Geochemistry, Geophysics, Geosystems*, *18*. https://doi.org/10.1002/2017GC007014

Received 9 MAY 2017
Accepted 16 NOV 2017
Accepted article online 22 NOV 2017

A Comparison of Geodetic and Geologic Rates Prior to Large Strike-Slip Earthquakes: A Diversity of Earthquake-Cycle Behaviors?

James F. Dolan[1] and Brendan J. Meade[2]

[1]Department of Earth Sciences, University of Southern California, Los Angeles, CA, USA, [2]Department of Earth and Planetary Sciences, Harvard University, Cambridge, MA, USA

Abstract Comparison of preevent geodetic and geologic rates in three large-magnitude (M_w = 7.6–7.9) strike-slip earthquakes reveals a wide range of behaviors. Specifically, geodetic rates of 26–28 mm/yr for the North Anatolian fault along the 1999 M_W = 7.6 Izmit rupture are ~40% faster than Holocene geologic rates. In contrast, geodetic rates of ~6–8 mm/yr along the Denali fault prior to the 2002 M_W = 7.9 Denali earthquake are only approximately half as fast as the latest Pleistocene-Holocene geologic rate of ~12 mm/yr. In the third example where a sufficiently long pre-earthquake geodetic time series exists, the geodetic and geologic rates along the 2001 M_W = 7.8 Kokoxili rupture on the Kunlun fault are approximately equal at ~11 mm/yr. These results are not readily explicable with extant earthquake-cycle modeling, suggesting that they may instead be due to some combination of regional kinematic fault interactions, temporal variations in the strength of lithospheric-scale shear zones, and/or variations in local relative plate motion rate. Whatever the exact causes of these variable behaviors, these observations indicate that either the ratio of geodetic to geologic rates before an earthquake may not be diagnostic of the time to the next earthquake, as predicted by many rheologically based geodynamic models of earthquake-cycle behavior, or different behaviors characterize different fault systems in a manner that is not yet understood or predictable.

1. Introduction

Geodetic observations of time-dependent surface deformation throughout an earthquake cycle can constrain physical models of fault loading and rates of elastic strain accumulation. Unfortunately, these data are not yet generally extant along most faults that are capable of generating $M_W > 7$ earthquakes due to long (>100 year) interevent times that exceed the duration of the observational epoch. However, geodetic observations immediately prior to large ($M_W \geq 7.6$) earthquakes are now available along the North Anatolian, Denali, and Kunlun strike-slip faults. While short of spanning a complete earthquake cycle, these decadal pre-earthquake measurements do provide constraints late in the earthquake cycle where differences between long-term geologic fault slip rates and geodetically inferred slip-deficit rates are predicted to be greatest (Hetland & Hager, 2006). Earthquake-cycle models of periodic earthquakes within an elastic upper crust coupled to a linear viscoelastic mantle (Cohen, 1982; Hetland & Hager, 2006; Savage & Prescott, 1978) predict relatively low near-fault velocity gradients in fault-parallel surface velocities prior to periodic main shock ruptures. This is the case when either lower crustal viscosities are low or earthquake recurrence times are long, and where viscoelastic processes are responsible for postseismic relaxation. Interpreted in the context of classical elastic dislocation models (Savage & Burford, 1973), these velocities would yield relatively slow slip-deficit rate estimates as compared with longer-term (10^4 to 10^5 years) geologic slip rate estimates. It is for this reason that GPS observations of the surface velocity field late in the earthquake cycle provide strong constraints on viable earthquake-cycle models.

In this paper, we summarize available geodetic and geologic rate data from the only three large-magnitude (M_W = 7.6–7.9) strike-slip earthquakes for which both sufficiently long preevent geodetic time series and well-constrained geologic fault slip rates are available. We discuss these results in terms of their implications for our understanding of fault mechanics, earthquake-cycle modeling, and the use of geologic and geodetic rate data in probabilistic seismic hazard assessment, and conclude by outlining some potential mechanisms that may explain the observed behaviors.

2. Observations of Geodetic and Geologic Rates Prior to Large-Magnitude Strike-Slip Earthquakes

2.1. 1999 Izmit, Turkey, Earthquake (North Anatolian Fault, Northern Strand)

The 1999 $M_W = 7.6$ Izmit earthquake was generated by rupture of 145 km of the main, northern strand of the North Anatolian fault (NAF-N; Barka, 1999; Barka et al., 2002; Reilinger et al. 2000), which accommodates most of the slip along the NAF system in northwestern Turkey (e.g., Barka, 1992; Hubert-Ferrari et al., 2002). Although fault slip along the NAF-N within the central Marmara Sea region to the west of the 1999 rupture may involve significant distributed deformation (e.g., Hergert & Heidbach, 2010), several well-constrained offsets from both the east and west of the central Marmara zone of structural complexity all yield NAF-N slip rates of ~15–20 mm/yr, over a wide range of time scales (<1,000 years to 500 ka; Dolan, 2009; Grall et al., 2013; Kurt et al., 2013; Meghraoui et al., 2012; Pucci et al., 2007).

These geologic rates are slower than geodetically constrained slip-deficit rates based on pre-1999 earthquake GPS data (Figure 1). For example, modeling of the 1988–1997 geodetic data suggests slip-deficit rates for the NAF-N strand of 24–30 mm/yr (e.g., Meade et al., 2002; Nyst & Thatcher, 2004; Reilinger et al., 2006; DeVries et al., 2016). Although the earlier block models were based on the assumption of internally rigid blocks, which could result in artificially rapid estimates of slip-deficit rates at block boundaries (i.e., the modeled faults), and some used block boundaries that did not exactly match the active strands of the NAF system in northwestern Turkey (as noted by Floyd et al., 2010), DeVries et al. (2016) used a geologically accurate, three-dimensional earthquake-cycle model that incorporates realistic block boundaries corresponding to the main, northern NAF-N strand, as well as the central NAF and southern NAF strands. Moreover, their model allows internal block strain and accounts for interseismic strain accumulation and viscoelastic deformation generated from ~500 years of $M_W > 6.5$ earthquakes. The DeVries et al. (2016) model yields a pre-1999 Izmit earthquake geodetic slip-deficit rate for the NAF-N strand rate in northwestern Turkey of 26–28 mm/yr, similar to the earlier-determined rates, and ~40% faster than the geologic slip rate (Figure 1).

This geologic-geodetic rate discrepancy could potentially be explained by distributed geologic deformation that is not accounted for in the fault offset measurements used to constrain geologic slip rates (e.g., Hergert & Heidbach, 2010). This hypothesis, however, is inconsistent with late Pleistocene to Holocene (10^4 to 10^5 years) geologic slip rate estimates (Dolan, 2009; Grall et al., 2013; Kozacı et al., 2009; Kurt et al., 2013; Meghraoui et al., 2012; Pucci et al., 2007; Rockwell et al., 2009) that come from both to the east and west of the central Marmara region zone of structural complexity at locations where the NAF-N is single stranded. For example, to the west of the central Marmara, studies by Rockwell et al. (2009; $15.8^{+7.3}/_{-3.8}$ mm/yr), Meghraoui et al. (2012; 17 ± 5 mm/yr), and Grall et al. (2013; 17.4 ± 2.3 mm/yr) yield rates that are similar to NAF-N rates measured to the east by Pucci et al. (2007; 15.0 ± 3.2 mm/yr), Dolan (2009; 16 ± 2 mm/yr), and Kurt et al. (2013; $18.5^{+10.9}/_{-5.9}$ mm/yr). Moreover, the similar, longer-term (100–500 ka) geologic slip rate estimates by Grall et al. (2013) and Kurt et al. (2013) are based on offsets of km-scale features and therefore likely incorporate any off-fault distributed deformation. Thus, the apparent geologic-geodetic rate discrepancy along the northern strand of the NAF-N is real, with the pre-Izmit earthquake slip-deficit rate being ~40% faster than the longer-term geologic fault slip rate (Figure 1).

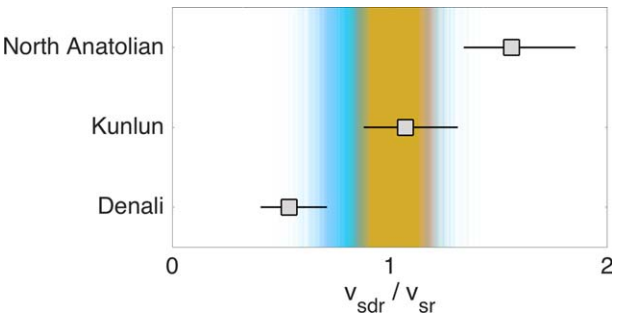

Figure 1. Comparison of geologic and geodetic rate data for the three earthquakes we discuss. Dots show ratios of long-term (10^4 to 10^5 years) average fault slip rates with geodetic rates immediately prior to the earthquakes. Denisty of blue and brown vertical lines show probability distribution functions of geologic-geodetic ratios from Meade et al. (2013) and Thatcher (2009), respectively. Note that rate of elastic strain accumulation along the Denali fault was only about half as fast as the long-term rate prior to the 2002 earthquake, whereas the rate of elastic strain accumulation on the NAF-N prior to the 1999 $M_W = 7.6$ Izmit earthquake was ~150% the long-term average slip rate; the ~1:1 geologic-geologic ratio prior to the 2001 $M_W = 7.8$ Kokoxili earthquake is similar to the near-1:1 ratios documented for many faults by Meade et al. (2013; blue lines in figure 1 [0.94%]) and Thatcher (2009; brown lines in Figure 1 [0.98%]).

2.2. 2001 Kokoxili, Tibet, Earthquake (Kunlun Fault)

The 2002 $M_W = 7.8$ Kokoxili rupture extended for more than 400 km along the central and western Kunlun fault in Tibet (Klinger et al., 2005; Lasserre et al., 2005; Van der Woerd et al., 2002a; Xu et al., 2002). Van Der Woerd et al. (2002b) documented Holocene slip rates at three sites along the west-central Kunlun fault, near 94°E, along the eastern part of the 2001 rupture. These rates yield a relatively consistent slip rate that averages 11.6 ± 1.5 mm/yr. The true rate could be somewhat

slower if upper terrace reconstructions of their offsets are considered (e.g., Cowgill, 2007); Van Der Woerd et al. (2002b) assumed only lower terrace reconstructions, which will yield maximum rates.

The ~N-S transect of GPS stations used to constrain the pre-Kokoxili velocity field crosses the Kunlun fault near 94°E, along the same stretch of the Kunlun fault from which Van der Woerd et al. (2002b) measured the geologic rates described above. Both time-independent (Meade, 2007) and time-dependent (DeVries & Meade, 2013; Hilley et al., 2005) slip-deficit rate estimates of these data yield estimates of 9–12 mm/yr. Thus, the geodetic and geologic data, collected from the same stretch of the central Kunlun fault, suggest that the pre-earthquake slip-deficit rate and the longer-term Holocene fault slip rate are similar at ~11 mm/yr (Figure 1).

2.3. 2002 Denali, Alaska, Earthquake (Denali and Totschunda Faults)

The 2002 $M_W = 7.9$ Denali earthquake initiated on the Sutsitna Glacier reverse fault and propagated for >350 km along the right-lateral Denali and Totschunda faults (Eberhart-Phillips et al., 2003). Matmon et al. (2006) documented the latest Pleistocene-Holocene average slip rate of the Denali fault at several sites along and to the east of the 2002 rupture. The Denali fault slip rate at their DFCR site (145°W) along the west-central part of 2002 rupture is particularly well constrained. At that site, they dated a clear 144 ± 14 m offset of a glacial moraine with ^{10}Be samples from both boulder tops and sediments. These age data yielded a well-constrained latest Pleistocene-Holocene (12 ka) slip rate of 12.1 ± 1.7 mm/yr.

The Matmon et al. (2006) DFCR geologic slip rate site is very close to the fault crossing of the Richardson Highway GPS transect detailed in Freymueller et al. (2008). As with the Izmit and Kokoxili geodetic data described above, a key aspect of these geodetic data is that a well-constrained time series is available from prior to the 2002 rupture. These prerupture geodetic data have been used to estimate a time-independent slip-deficit rate of 6–8 mm/yr (Freymueller et al., 2008). Thus, the geodetic slip-deficit rate on the Denali fault prior to the 2002 earthquake was only about half of the Holocene geologic slip rate (Figure 1).

3. Discussion

3.1. A Diversity of Earthquake-Cycle Behaviors

The comparisons above reveal a diversity of earthquake-cycle behaviors, with geodetic slip-deficit rates that are faster than, slower than, and similar to longer-term geologic average rates prior to the 1999 Izmit, 2002 Denali, and 2001 Kokoxili earthquakes, respectively. This diverse range of behaviors is not consistent with classical two-layer Maxwell rheology earthquake-cycle models (e.g., Savage & Prescott, 1978). In particular, this class of earthquake models predicts that geodetically constrained slip-deficit estimates late in the earthquake cycle should be slower than the geologic rate at the end of a strain-accumulation cycle in the limit that earthquake recurrence intervals are relatively long (e.g., >500 years) and/or sub-upper crustal viscosities are relatively low (e.g., $<10^{18}$ Pa s; e.g., Savage, 2000; Savage & Prescott, 1978). This type of behavior is consistent with the much slower geodetic slip-deficit rate estimates from prior to the 2002 Denali earthquake relative to geologic rate estimates.

Observational evidence for this behavior is sparse, however (Meade et al., 2013). More commonly, geodetic-geologic rate comparisons spanning various points in the earthquake cycles of many faults yield similar rates (0.94 ± 0.09 Pearson correlation coefficient), such as occurred prior to the 2001 Kokoxili earthquake on the Kunlun fault (Meade et al. 2013; Thatcher, 2009). This similarity between geologic and geodetic rates, in addition to the observation of rapid postseismic deformation rates, can be explained by earthquake-cycle models that include multiple relaxation time scales (DeVries & Meade, 2013; Hetland & Hager 2006). In contrast, we are not aware of extant mechanical models models that can explain the faster-than-average slip-deficit rate estimates constrained by GPS observations from late in the earthquake cycle, as was the case prior to the 1999 Izmit rupture.

3.2. Possible Explanations

Here we consider several possible mechanisms that may provide testable hypotheses concerning the controls on the observed behaviors. Specifically, we consider four possible mechanisms—two related to intrinsic behavior of the fault zone, and two associated with extrinsic controls—that could potentially explain these observations: (1) earthquake-cycle effects related to previous clusters or lulls in earthquake

occurrence and fault displacement; (2) temporal variability in fault strength; (3) regional kinematic fault interactions; and (4) temporal variability of relative plate motion rates.

3.2.1. Effects of Temporal Clustering of Large Earthquakes

Earthquake-cycle models that include the effects of temporal clusters of large-displacement ruptures suggest that geodetic rates at the end of a strain-accumulation cycle could be slightly faster than the cycle average rate following such a cluster (Meade & Hager, 2004). Could this explain, for example, the elevated geodetic slip-deficit rate observed along the future rupture zone of the 1999 Izmit earthquake? Historical and paleoseismic data from the region suggest not. In fact, these observations are consistent with the idea that earthquake recurrence along this stretch of the main, northern strand of the NAF is notably regular, with major prior events occurring approximately every 200–300 years for at least the past several cycles (e.g., 1912 and 1999 events, 1719–1766 sequence, 1509 earthquake, and fourteenth and eleventh century events; Ambraseys, 1970, 2002; Ambraseys & Finkel, 1995; Barka, 1992; Hubert-Ferrari et al., 2000; Klinger et al., 2003; Kozacı et al., 2011; Rockwell et al., 2009); Rockwell et al. (2009), for example, suggested an average recurrence interval of 283 ± 113 years for the NAF-N west of the Marmara region for the past millennium. In the case of the Izmit area, it is possible that the 1894 Marmara earthquake ($M \sim 7.3$; Ambraseys, 2001) could have occurred on or near the NAF-N strand just west of the Izmit rupture. But even if this is the case, that event occurred more than 100 years before the Izmit rupture. Moreover, occurrence of the 1894 event cannot explain the observed faster pre-earthquake NAF-N slip-deficit rates along the central and eastern parts of the Izmit rupture, as well as the section of the fault extending for $\geq$50 km to the east of the Izmit rupture, all of which lie well to the east of the possible rupture area of the 1894 earthquake. Thus, the apparently elevated rate of elastic strain accumulation along this section of the NAF just prior to the 1999 Izmit rupture cannot be explained by earthquake clustering.

Conversely, an anomalously long lull in earthquake recurrence could lead to geodetic slip-deficit rates at the end of a strain-accumulation cycle that are slower than the expected average rate for an individual earthquake cycle (Meade & Hager, 2004). This effect cannot explain the slower-than-average slip-deficit rate just prior to the 2002 Denali earthquake, however, because historical data and field observations show that slip along the western part of the Denali rupture in the vicinity of the geodetic and geologic rate data we consider generated the 1912 $M \sim 7.3$ Delta Valley earthquake (Carver et al., 2004), whereas the penultimate event farther east along the Denali fault occurred $\sim$600–800 years ago (Schwartz et al., 2012). Thus, the slow rate of elastic strain accumulation observed along the Denali fault prior to the 2002 earthquake cannot be ascribed to an anomalously long pre-2002 event lull in fault slip.

3.2.2. Temporal Variations in Fault Strength

Could the range of behaviors we observe reflect changes in fault strength through time? Incremental geological fault slip-rate records from major strike-slip faults reveal that in at least some cases, fault displacement through time can vary by $\geq$500% over sequences that span multiple earthquake cycles (e.g., Dawson et al., 2003; Dolan et al., 2016; Gold & Cowgill, 2011; Hatem et al., 2016; Mason et al., 2004, 2006; Weldon et al., 2004; Zinke et al., 2017). Moreover, such irregular slip behavior may extend to even longer time and displacement scales (e.g., Marco et al., 1996). Although geological data cannot directly measure paleoelastic strain accumulation rates, such extreme variations in fault slip rate spanning multiple earthquake cycles suggest the possibility that the rate of elastic strain accumulation along faults may also vary significantly through time. For example, in the San Andreas fault (SAF) earthquake record at Wrightwood (Weldon et al., 2004), there are alternating, 3- to 5-earthquake-long "fast" and "slow" periods of slip, during each of which the rate of fault slip remains relatively constant (Dolan et al., 2016). This pattern is consistent with the hypothesis that the SAF may "keep up" with a temporally variable fault-loading rate within each of the 3–5-earthquake strain super-cycles (Dolan et al., 2016).

Previous suggestions of mechanisms that could result in temporally variable strain accumulation and release along faults have included alternate strengthening and weakening of faults, either through changes in normal stress and/or changes in the strength of fault-zone rocks themselves (e.g., Chery & Vernant, 2006; Dolan et al., 2007, 2016; Hetzel & Hampel, 2005; Luttrell & Sandwell, 2010; Oskin et al., 2008). We discuss both possibilities below.

Stress-related changes due to addition or removal of gravitational loads. For example, Luttrell and Sandwell (2010) calculated the effects of rising sea level on the stresses acting on several fault systems. They found that as sea level rises, normal stresses acting on coast-parallel faults will either strengthen or weaken,

depending on fault location, as the gravitational load is redistributed. In the case of the North Anatolian fault, they showed that the normal stresses acting on the fault were reduced as the level of the Black Sea rose in the early Holocene, promoting failure. Could this explain the observed discrepancy between geodetic and geologic rates along the NAF? Available data suggest not. Specifically, Yanchilina et al. (2017) show that the level of the Black Sea rose abruptly by $\geq$120 m as the previously brackish lake filling the deeper parts of the basin filled within a few decades $\sim$9.3 ka, when the Bosporus sill was breached by Mediterranean sea water. Thus, any major stress-related changes to the strength of the NAF would have occurred during the early Holocene, with little subsequent change during the past $\sim$9 kyr (Luttrell & Sandwell, 2010). Inasmuch as the compilation of NAF slip rates by Kozacı et al. (2009) reveals relatively constant slip rates along the NAF spanning a wide range of time periods, from 2 to $>$100 ka, this does not seem to provide a ready explanation for the observed geodetic-geologic rate discrepancy. Indeed, the fastest well-constrained geologic slip rate for the NAF is based on restoration of a late Holocene (2 ka) datum (Kozacı et al., 2007).

Luttrell and Sandwell (2010) also showed that early Holocene sea level rise reduced the normal stress acting on the Denali fault, potentially increasing slip on the seismogenic part of the fault. As noted above, the Denali fault geologic slip rate (Matmon et al., 2006) is based on restoration of 12 ka offsets, and thus would encompass any period of potentially faster fault slip rate associated with sea level rise, consistent with the observed geodetic-geologic rate discrepancy. However, any potential normal stress-induced changes in slip rate would have occurred during a relatively brief part of the 12,000 year-long period over which this slip rate is averaged, during the early Holocene when most sea level rise occurred. Thus, although this could potentially contribute to the geodetic-geologic rate discrepancy observed prior to the 2002 Denali earthquake, we think it is unlikely to fully explain the discrepancy.

Similarly, any potential ice removal during latest Pleistocene-Holocene glacier retreat would also reduce the normal stresses acting on the Denali fault at depth, thus weakening the fault and promoting failure, potentially leading to faster geologic slip rates. However, the strength of deep, downdip extensions of the Alaska megathrust beneath southern Alaska (and the Denali fault) would also be reduced during sea level rise (e.g., Luttrell & Sandwell, 2010), and the potential interactions between fault strength in both the upper, brittle faults and the deep, ductile downdip extensions of both the Denali fault and the Alaska subduction megathrust need to be investigated to determine the relative effects of such gravitational stress redistribution effects on both the seismogenic parts of these faults and their downdip ductile roots.

Changes in fault strength due to changes in fault-zone rock physical properties. Alternatively, temporal variations in the strength of fault-zone rocks in the ductile roots of major faults may influence temporally irregular fault slip rates. For example, Dolan et al. (2007, 2016) suggested that the ductile roots of a fault could harden during periods of anomalously rapid fault slip, with strain hardening processes occurring at rates that temporarily overwhelm counteracting annealing processes. In their model, this leads to a lull in ductile shear, and consequently in upper crustal strain accumulation and earthquakes. They suggested that during such lulls, plate boundary strain is accommodated preferentially on other faults, and the fault experiencing the lull (i.e., slow/no slip rate) gradually weakens as a result of annealing, weakening the fault and increasing ductile shear and geodetic slip-deficit rates. Another possibility is that this behavior may be driven by the (random) occurrence of the first event in an earthquake cluster, which may serve to somehow weaken the ductile shear zone below the fault. For example, Oskin et al. (2008) suggested that the first earthquake in a cluster might release fluids downward into the ductile roots of the fault zone, weakening it and allowing faster creep rates, which in turn would drive faster elastic strain accumulation in the upper crust and more frequent earthquakes. Both of these potential mechanisms are consistent with the ductile roots of major faults being mechanically stronger during lulls and weaker at the onset of and/or during a cluster. Both of these suggested mechanisms are problematic, however. The latter would require that fault-zone fluids travel downward within the shear zone, opposite to generally upward-decreasing pressure gradients, and the former would seem most likely to operate at relatively low temperatures and high stresses such as those that would be most likely to be encountered in the shallow levels of ductile shear zones, just below the brittle-ductile transition.

Moreover, in order to yield geodetic signals that would be interpreted as either anomalously slow or fast elastic strain accumulation along a fault, mechanisms that invoke alternate strengthening and weakening on ductile shear zones would have to affect the entire shear zone to depths of at least 60–80 km (Figure 2). Thus, for such mechanisms to explain, for example, the anomalously rapid geodetic slip-deficit rate prior to

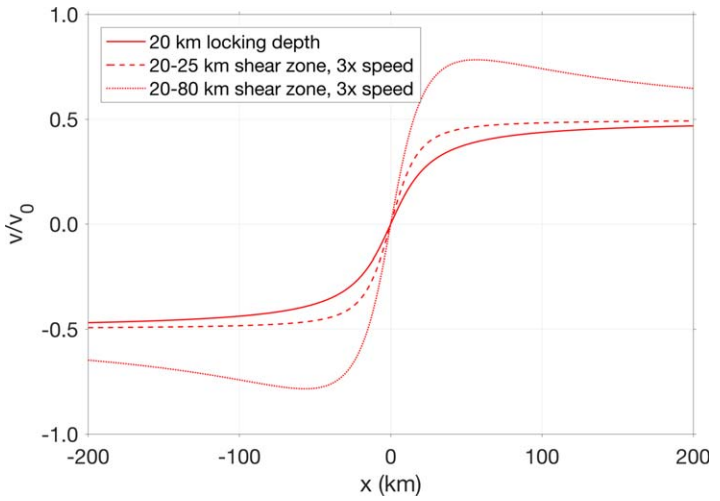

Figure 2. Expected surface velocity profiles for faults that are (a) locked down to 20 km depth and slipping at average rate below (solid line); (b) locked to 20 km depth, but slipping 3X faster than average from 20 to 25 km depth (dashed line); and (c) locked from surface to 20 km depth and slipping at 3X average rate for a shear zone extending from 20 to 80 km depth (dotted line). Only the deep shear-zone model yields far-field rates that would be interpreted as a slip-deficit rate that is faster than average.

the 1999 Izmit earthquake would require that deep, localized shear in the lowermost crust and uppermost mantle below the locked seismogenic part of the fault was occurring at rates faster than the long-term fault slip rate during the late stages of the earthquake cycle.

How might this occur? It is possible that mechanisms such as shear heating and associated fluid movements could cause changes in the physical properties of the ductile shear-zone rocks that could contribute to understanding the observed rate changes. Periods of anomalously rapid slip within ductile shear zones would generate additional shear heat (e.g., Leloup et al., 1999; Thatcher & England, 1998; Takeuchi & Fialko, 2012), which in turn could drive dehydration reactions within shear-zone rocks. Dehydration reactions could potentially explain a hardening of the shear-zone rocks that were initially shearing rapidly, and some studies have suggested that this will result in movement of the fluids laterally into shear-zone wall rocks, which will consequently weaken and therefore increase the overall width of the ductile shear zone (e.g., Finch et al., 2016; Oliot et al., 2014), rather than slow the rate of overall shear. Although local outward migration of fluids almost certainly occurs (e.g., Finch et al., 2016), analyses of fluid content in the high-strain ultra-mylonite cores of ductile shear zones reveal a range of fluid contents relative to wall rocks (e.g., Finch et al., 2016; Kronenberg et al., 1990; Kronenberg & Wolf, 1990; Oliot et al., 2010, 2014), suggesting that there are multiple processes at work that may not be fully understood.

We consider the concept that if the fluids released by these dehydration reactions diffuse upward, in response to a pressure gradient related to their higher temperatures, rather than exclusively outward, this could potentially provide a means of strengthening the ductile shear-zone rocks, thus slowing the overall rate of slip of the shear zone if the entire width of the shear zone was affected over a large depth extent. But for fault strength variations to explain the observed range of behaviors requires a mechanism in which the fault alternates between strengthening and weakening, with attendant changes in ductile shear-zone rate. How might the ductile shear zone then "switch back on"? We suggest that fluids from water-bearing shear-zone wall rocks will gradually diffuse back into the dewatered, hardened shear-zone rocks with time in response to the chemical potential gradient resulting from the disequilibrium created by this juxtaposition. The gradual reintroduction of water into the ductile shear-zone rocks will weaken them, thus potentially increasing the rate of shear across the ductile fault zone, completing the "fast-slow" cycle we suggest. The time scales over which this diffusive rehydration could potentially occur could be quite long, however, potentially much longer than the centennial to millennial periods of temporally variable slip rate observed in some paleoseismic studies, especially at the relatively low temperatures ($<$500°C) that characterize the shallowest parts of ductile shear zones below the brittle-ductile transition in the lower midcrust. Nevertheless, we suggest that the possibility that such processes and feedbacks could occur in ductile shear zones is worth additional investigation, particularly in terms of the time scales involved in alternately dehydrating, then rehydrating fault-zone rocks, especially within the fine-grained ultra-mylonitic rocks that form the high-strain cores of many shear zones.

3.2.3. Regional Fault Kinematic Controls

Alternatively, could interactions among kinematically and geometrically variable faults in structurally complex plate boundary fault systems induce changes in fault loading and slip rates? Specifically, could these interactions and associated changes in stressing rate induced on one fault by variations in slip rate on another fault influence the rate of elastic strain accumulation and release along other faults in the system (e.g., Gabrielov et al., 1996)?

In one possible example of such behavior, it has long been noted that in the Mojave region north of Los Angeles in California geodetic slip-deficit rates along the conjugate San Andreas and Garlock faults are slower than longer-term geologic slip rates (e.g., Dolan et al., 2007, 2016; Ganev et al., 2012; Meade & Hager, 2005; McGill et al., 2009; Peltzer et al., 2001). Conversely, slip-deficit rates measured across the mechanically

complementary faults of the eastern California shear zone (ECSZ) are faster than the collective geologic slip rate across that system (Dolan et al., 2007; Meade & Hager, 2005; Oskin et al., 2008; Oskin & Iriondo, 2004; Peltzer et al., 2001), although this discrepancy may be reduced somewhat when off-fault deformation not accounted for in the geologic rates is considered (Dolan & Haravitch, 2014; Milliner et al., 2016). Dolan et al. (2007, 2016) suggested that these observations could be explained by a kinematic model in which the conjugate San Andreas-Garlock fault system and the mechanically complementary ECSZ "trade off" accommodating Pacific-North America relative plate motion. Using available geodetic and geologic rates, they suggested that the faults of the ECSZ are currently storing and releasing energy faster than average, while the San Andreas-Garlock part of the system is storing and releasing energy more slowly than average.

Could such interactions among upper crustal faults explain the wide range of behaviors we discuss for the Izmit, Kokoxili, and Denali earthquakes? The causative faults for these three earthquakes—the northern strand of the North Anatolian fault, the Kunlun fault, and the Denali fault, respectively—are by far the fastest-slipping strike-slip faults in their respective regions, and thus their behavior, rather that that of nearby upper crustal secondary faults, would seem most likely to dominate the behavior of the region in which they reside. Nevertheless, as with almost all major faults, the three faults we consider are components of much larger, mechanically integrated fault systems that serve to accommodate relative plate boundary motion, and are thus subject to far-field "extrinsic" controls on their behavior.

For example, as noted above, the Denali fault lies above and north of the north-dipping subduction megathrust fault, which ruptured most recently in the 1964 $M_W = 9.2$ Alaska earthquake. Could stress interactions associated with the 1964 earthquake account for the observed geodetic-geologic rate discrepancy prior to the 2002 Denali earthquake? Stress modeling suggests not. Specifically, although Coulomb Failure Function modeling by Bufe and Boyd (2008) showed that the 1964 earthquake reduced the normal stress acting on the Denali fault, which would favor faster slip rates along the upper plate Denali strike-slip fault, the geologic slip rate used in our comparison is averaged over 12,000 years, making it unlikely that any minor Denali fault slip-rate acceleration induced by the 1964 earthquake could explain the approximately 2:1 discrepancy between the geodetic and geologic rates prior to the 2002 Denali earthquake. Moreover, the ongoing geodetic signal of deep afterslip on the 1964 rupture plane (Freymueller et al., 2008) would have served to reduce normal stresses acting on any deep ductile extensions of the Denali fault prior to the 2002 earthquake. Although ductile shear is relatively insensitive to changes in normal stress (e.g., Sammis et al., 1977), the resulting decrease in normal stress would seem to favor slightly increased—not decreased—rates of elastic strain accumulation along the Denali fault, opposite to the observed geodetic-geologic rate discrepancy. It is worth noting, however, that potential interactions between changes in normal stress that may inhomogeneously affect shear-zone rocks and wall rocks with different material properties, and the lateral influx of fluids into the shear zone and resulting shear-zone weakening, remain poorly understood and require further investigation.

3.2.4. Possibility of Temporally Variable Plate Rates

Temporally variable tectonic plate motions may also contribute to explaining the diversity of behaviors observed late in the earthquake cycle. Plate velocities constrained by decade-long GPS time series are in most cases similar to global plate motion models based on 3 Ma magnetic anomalies (e.g., DeMets et al., 1994; Sella et al., 2002), and there is a tacit assumption in most geodynamical studies that overall plate rates do not change significantly on intermediate time scales absent some major change in plate boundary configuration (e.g., ongoing collisional slowing; Sella et al., 2002). But what if this assumption is incorrect? Both coseismically induced stress changes (Anderson, 1975; Romanowicz, 1993) and geometric inconsistencies (Gabrielov et al., 1996) may allow plates to change motion over earthquake-cycle and possibly longer time scales (Ismail-Zadeh et al., 1999, 2007). The central idea being that perturbations at the edges of tectonic plates may be large enough to require a change in plate motions in order to satisfy the force balance. Conditions necessary for this sort of behavior to exceed the 1 mm/yr level include relatively low mantle viscosities (10^{19} Pa s), small block dimensions (<500 km radius), and cumulative earthquake stress changes of $>10^3$ Pa (Meade & Loveless, 2017). Applied to the geologic slip rate and geodetic slip-deficit rates considered here, an explanation for the diversity of pre-earthquake slip-deficit rates might be that the relative motions between the tectonic plates on either side of the fault vary at time scales less than the averaging time scale over which geologic slip rate estimates are constrained.

It is interesting that in the two examples we discuss that exhibit slip-deficit rates that are markedly different from longer-term geologic rates (Denali fault and NAF-N), the causative faults are parts of regional fault

systems that are kinematically linked to nearby subduction zones (the Alaskan subduction zone and the Hellenic trench, respectively). Could interactions with temporally anomalous slip along the megathrusts, perhaps along their downdip extensions, explain the observations? For example, could anomalously rapid aseismic slip along the Hellenic subduction megathrust perhaps accelerate the slip-deficit rates along the faults of the western NAF system? Notably, models of geodetic data suggest that the NAF-N strand slip-deficit rate increases markedly westward from ~31.5°E (e.g., DeVries et al., 2016), suggesting that these elevated rates may be related to potentially transient behavior of western Anatolia and the Aegean region to the west, perhaps in response to transient slip along the Hellenic subduction zone. Such transient subduction megathrust slip may be difficult to discern. Meade and Loveless (2009), for example, showed that the geodetic signal of long-lived (decades to centuries) slow slip events may never exceed the plate convergence rate and thus may not be readily distinguishable from signals that are usually interpreted as evidence for partial elastic coupling on subduction megathrusts.

In the case of the 2002 Denali earthquake, as noted above the effects of long-lived deep afterslip on the underlying subduction megathrust observed geodetically (Freymueller et al., 2008) would most likely reduce normal stresses acting on the Denali fault. If this normal stress decrease had any effect on the rate of elastic strain accumulation along the Denali fault, it may have increased, rather than decreased, the elastic strain accumulation rate on the Denali fault. This is opposite to the observed geodetic-geologic rate discrepancy, so cannot explain the observations.

4. Conclusions and Implications

Comparison of geodetic and geologic rates immediately prior to the 1991 $M_W = 7.6$ Izmit, 2001 $M_W = 7.8$ Kokoxili, and 2002 $M_W = 7.9$ Denali strike-slip earthquakes reveals a complete range of pre-earthquake rate ratios, with geodetic rates that are faster than, similar to, and slower than the geologic fault slip rates. The range of behaviors revealed by these three earthquakes—the only three large-magnitude strike-slip examples we are aware of that have both pre-event GPS time series and well-constrained geologic slip rates—demonstrates that there is a not a single relationship between geodetic and geologic rate data that can be applied to all faults. Moreover, these results demonstrate that we do not yet understand fully the controls on patterns of elastic strain accumulation and release in large earthquakes on major faults, as no single mechanism can explain all of the observations. It is possible that these behaviors may be controlled by some complex interplay between multiple processes that may be specific to any individual fault, as well as by processes that are extrinsic to each particular fault. This reinforces the view that a true understanding of the geodynamics of fault behavior requires a system-level analysis. Indeed, by focusing on single faults to the exclusion of their tectonic context, one could miss the potentially rich range of controls and behaviors that may result from system-level interactions. Whether the controls on these behaviors are intrinsic to the fault (e.g., clusters and lulls in earthquake recurrence, or changes in fault-zone properties, either in upper crust or underlying ductile shear zones) or extrinsic (temporal changes in fault loading rates, either due to temporal variations in induced Coulomb stressing rate due to variable slip rates on other faults, or to centennial-millennial changes in plate rates), these observations demonstrate that no single existing earthquake-cycle model can provide an adequate description for the observed diversity of earthquake-cycle behaviors.

Acknowledgments
We thank Phoebe DeVries, Brad Hacker, and Charlie Sammis for helpful discussions, and Tim Wright and two anonymous reviewers for thoughtful comments on the manuscript. This work is partially an outgrowth of research conducted with support from U.S. National Science Foundation grants EAR-9980564 and EAR-0409767 (Dolan). All data used in this paper are available in the cited references.

References

Ambraseys, N. (1970). Some characteristics of the Anatolian fault zone. *Tectonophysics*, *9*, 143–165.
Ambraseys, N. (2001). The earthquake of 10 July 1894 in the Gulf of Izmit (Turkey) and its relation to the earthquake of 17 August 1999. *Journal of Seismology*, *5*(1), 117–128. https://doi.org/10.1023/A:1009871605267
Ambraseys, N. N. (2002). The seismic activity of the Marmara Sea region over the last 2000 years. *Bulletin of the Seismological Society of America*, *92*(1), 1–18.
Ambraseys, N. N., & Finkel, C. F. (1995). *The seismicity of Turkey and adjacent areas: A historical review, 1500–1800* (240 pp.). Istanbul, Turkey: Eren Yayincilik ve Kitapcilik Ltd Sti (Eren Press).
Anderson, D. L. (1975). Accelerated plate tectonics. *Science*, *187*, 1077–1079.
Barka, A., Akyüz, H. S., Altunel, E., Sunal, G., Cakir, Z., Dikbas, A., . . . Page, W. (2002). Surface rupture and slip distribution of the 17 August 1999 Izmit earthquake (Mw 7.4), North Anatolian fault. *Bulletin of the Seismological Society of America*, 92, 43–60.
Barka, A. A. (1992). The North Anatolian fault zone. *Anneles Tectonicae*, *6*, 164–195.
Barka, A. A. (1999). The 17 August 1999 Izmit Earthquake. *Science*, *285*, 1858–1859. https://doi.org/10.1126/science.285.5435.1858

Bufe, C. G., & Boyd, O. S. (2008). Fault interaction in Alaska: Static Coulomb stress transfer. In J. T. Freymueller, P. J. Haeussler, R. L. Wesson, & G. Ekström (Eds.), *Active tectonics and seismic potential of Alaska. Geophysical monograph series 179* (pp. 417–430). Washington, DC: American Geophysical Union. https://doi.org/10.1029/179GM24

Carver, G., Plafker, G., Metz, M., Cluff, L., Slemmons, B., Johnson, E., . . . Sorensen, S. (2004). Surface rupture on the Denali fault interpreted from tree damage during the 1912 Delta River *M*w 7.2–7.4 Earthquake: Implications for the 2002 Denali fault earthquake slip distribution. *Bulletin of the Seismological Society of America*, *94*, S58–S71.

Chery, J., & Vernant, P. (2006). Lithospheric elasticity promotes episodic fault activity. *Earth and Planetary Science Letters*, *243*, 2135–2144.

Cohen, S. C. (1982). A multilayer model of time dependent deformation following an earthquake on a strike slip fault. *Journal of Geophysical Research*, *87*, 5409–5421.

Cowgill, E. (2007). Impact of riser reconstructions on estimation of secular variation in rates of strike–slip faulting: Revisiting the Cherchen River site along the Altyn Tagh Fault, NW China. *Earth and Planetary Science Letters*, *254*, 239–255. https://doi.org/10.1016/j.epsl.2006.09.015

Dawson, T. E., McGill, S. F., & Rockwell, T. K. (2003). Irregular recurrence of paleoearthquakes along the central Garlock fault near El Paso Peaks, California. *Journal of Geophysical Research*, *108*(B7), 2356. https://doi.org/10.1029/2001JB001744

DeMets, C., Gordon, R. G., Argus, D. F., & Stein, S. (1994). Effect of recent revisions to the geomagnetic reversal time scale on estimates of current plate motions. *Geophysical Research Letters*, *21*, 2191–2194.

DeVries, P. M. R., Krastev, P. G., Dolan, J. F., & Meade, B. J. (2016). Viscoelastic block models of the North Anatolian fault: A unified earthquake cycle representation of pre- and postseismic geodetic observations. *Bulletin of the Seismological Society of America*, *107*, 403. https://doi.org/10.1785/0120160059

DeVries, P. M. R., & Meade, B. J. (2013). Earthquake cycle deformation in the Tibetan plateau with a weak mid-crustal layer. *Journal of Geophysical Research: Solid Earth*, *118*, 3101–3111. https://doi.org/10.1002/jgrb.50209

Dolan, J. (2009). Possible transient strain accumulation along the North Anatolian fault: Precursor or artifact? In *Proceedings of the international symposium on historical earthquakes and conservation of monuments and sites in the Eastern Mediterranean Region, 500th anniversary year of the 1509 September 10, Marmara Earthquake 10–12 September 2009* (extended abstract; 2 pp. I figure). Istanbul, Turkey: Istanbul Technical University.

Dolan, J. F., Bowman, D. D., & Sammis, C. G. (2007). Long-range and long-term fault interactions in southern California. *Geology*, *35*, 855–858.

Dolan, J. F., & Haravitch, B. D. (2014). How well do surface slip measurements track slip at depth in large strike-slip earthquakes? The importance of fault structural maturity in controlling on-fault slip versus off-fault surface deformation. *Earth and Planetary Science Letters*, *388*, 38–47. https://doi.org/10.1016/j.epsl.2013.11.043

Dolan, J. F., McAullife, L. J., Rhodes, E. J., McGill, S. F., & Zinke, R. (2016). Extreme multi-millennial slip rate variations on the Garlock fault, California: Strain super-cycles, potentially time-variable fault strength, and implications for system-level earthquake occurrence. *Earth and Planetary Science Letters*, *446*, 123–136. https://doi.org/10.1016/j.epsl.2016.04.011

Eberhart-Phillips, D., Haeussler, P. J., Freymueller, J. T., Frankel, A. D., Rubin, C. M., Craw, P., . . . Wallace, W. K. (2003). The 2002 Denali fault earthquake, Alaska: A large magnitude, slip-partitioned event. *Science*, *300*(5622), 1113–1118. https://doi.org/10.1126/science.1082703

Finch, M. A., Weinberg, R. F., & Hunter, N. J. R. (2016). Water loss and the origin of thick mylonites. *Geology*, *44*, 599–602. https://doi.org/10.1130/G37972.1

Floyd, M. A., Billiris, H., Paradissis, D., Veis, G., Avallone, A., Briole, P., . . . England, P. C. (2010). A new velocity field for Greece: Implications for the kinematics and dynamics of the Aegean. *Journal of Geophysical Research* , *115*, B10403. https://doi.org/10.1029/2009JB007040

Freymueller, J. T., Woodard, H., Cohen, S. C., Cross, R., Elliott, J., Larsen, C. F., . . . Zweck, C. (2008). Active deformation processes in Alaska, based on 15 years of GPS measurements. In J. T. Freymueller, P. J. Haeussler, R. L. Wesson, & G. Ekström (Eds.), *Active tectonics and seismic potential of Alaska. Geophysical monograph series 179* (pp. 1–42). Washington, DC: American Geophysical Union. https://doi.org/10.1029/179GM02

Gabrielov, A., Keilis-Borok, V., & Jackson, D. D. (1996). Geometric incompatibility in a fault system. *Proceedings of the National Academy of Sciences of the United States of America*, *93*, 3838–3842.

Ganev, P. N., Dolan, J. F., McGill, S. F., & Frankel, K. L. (2012). Constancy of geologic slip rate along the central Garlock fault: Implications for strain accumulation and release in southern California. *Geophysical Journal International*, *190*, 745–760. https://doi.org/10.1111/j.1365-246X.2012.05494.x

Gold, R., & Cowgill, E. (2011). Deriving fault-slip histories to test for secular variation in slip, with examples from the Kunlun and Awatere faults. *Earth and Planetary Science Letters*, *301*, 52–64. https://doi.org/10.1016/j.epsl.2010.10.011

Grall, C., Henry, P., Thomas, Y., Westbrook, G. K., Çağatay, M. N., Marsset, B., . . . Géli, L. (2013). Slip rate estimation along the western segment of the Main Marmara Fault over the last 405–490 ka by correlating mass transport deposits. *Tectonics*, *32*, 1587–1601. https://doi.org/10.1002/2012TC003255

Hatem, A. E., Dolan, J. F., Langridge, R. M., Zinke, R. W., McGuire, C. P., Rhodes, E. J., & Van Dissen, R. J. (2016). *Incremental slip rate and paleoseismic data from the eastern Hope fault, New Zealand: The Hossack and Green Burn sites*. Abstract T32B-07 presented at EOS transactions of the AGU, Fall Annual AGU Meeting, San Francisco, CA, December 12.

Hergert, T., & Heidbach, O. (2010). Slip-rate variability and distributed deformation in the Marmara Sea fault system. *Nature Geoscience*, *3*, 132– 135. https://doi.org/10.1038/ngeo739

Hetland, E., & Hager, B. (2006). Interseismic strain accumulation: Spin-up, cycle invariance, and irregular rupture sequences. *Geochemistry, Geophysics, Geosystems*, *7*, Q05004. https://doi.org/10.1029/2005GC001087

Hetzel, R., & Hampel, A. (2005). Slip rate variations on normal faults during glacial–interglacial changes in surface loads. *Nature*, *435*, 81–84.

Hilley, G. E., Bürgmann, R., Zhang, P.-Z., & Molnar, P. (2005). Bayesian inference of plastosphere viscosities near the Kunlun fault, northern Tibet. *Geophysical Research Letters*, *32*, L01302. https://doi.org/10.1029/2004GL021658

Hubert-Ferrari, A., Armijo, R., King, G., Meyer, B., & Barka, A. A. (2002). Morphology, displacement, and slip rates along the North Anatolian fault, Turkey. *Journal of Geophysical Research*, *107*(B10), 2235. https://doi.org/10.1029/2001JB000393

Hubert-Ferrari, A., Barka, A., Jacques, E., Nalbant, S. S., Meyer, B., Armijo, R., .. King, G. C. P. (2000). Seismic hazard in the Marmara Sea region following the 17 August 1999 Izmit earthquake. *Nature*, *404*(6775), 269–273.

Ismail-Zadeh, A., Keilis-Borok, V. I., & Soloviev, A. A. (1999). Numerical modelling of earthquake flow in the southeastern Carpathians (Vrancea): Effect of a sinking slab. *Physics of the Earth and Planetary Interiors*, *1113*), 267–274.

Ismail-Zadeh, A., Le Mouël, J. L., Soloviev, A., Tapponnier, P., & Vorovieva, I. (2007). Numerical modeling of crustal block-and-fault dynamics, earthquakes and slip rates in the Tibet-Himalayan region. *Earth and Planetary Science Letters*, *258*, 465–485. https://doi.org/10.1016/j.epsl.2007.04.006

Klinger, Y., Sieh, K., Altunel, E., Akoglu, A., Barka, A., Dawson, T., . . . Rockwell, T. (2003). Paleoseismic evidence of characteristic slip on the western segment of the North Anatolian fault, Turkey. *Bulletin of the Seismological Society of America*, *93*, 2317–2332. https://doi.org/10.1785/0120010270

Klinger, Y., Xu, X., Tapponnier, P., Van Der Woerd, J., Lasserre, C., & King, G. C. P. (2005). High-resolution satellite imagery mapping of the surface rupture and slip distribution of the Mw 7.8, November 14, 2001 Kokoxili earthquake (Kunlun fault, northern Tibet, China). *Bulletin of the Seismological Society of America*, *95*(5), 1970–1987.

Kozacı, Ö., Dolan, J. F., & Finkel, R. C. (2009). A late Holocene slip rate for the central North Anatolian fault, at Tahtakörprü, Turkey, from cosmogenic ^{10}Be geochronology: Implications for fault loading and strain release rates. *Journal of Geophysical Research*, *114*, B01405. https://doi.org/10.1029/2008JB005760

Kozacı, Ö., Dolan, J. F., Finkel, R. C., & Hartleb, R. D. (2007). A 2000-year slip rate for the North Anatolian fault, Turkey, from cosmogenic ^{36}Cl geochronology: Implications for the constancy of fault loading and slip rates. *Geology*, *35*, 867–870. https://doi.org/10.1130/G23187A.1

Kozacı, Ö., Dolan, J. F., YÖnlü, Ö., & Hartleb, R. D. (2011). Paleoseismologic evidence for the relatively regular recurrence of infrequent, large-magnitude earthquakes on the eastern North Anatolian fault at Yaylabeli, Turkey. *Lithosphere*, *3*, 37–54. https://doi.org/10.1130/L118.1

Kronenberg, A. K., Segall, P., & Wolf, G. H. (1990). Hydrolytic weakening and penetrative deformation within a natural shear zone. In A. G. Duba et al. (Eds.), *The brittle-ductile transition in rocks: The heard volume. Monograph 56* (pp. 21–36). Washington, DC: American Geophysical Union. https://doi.org/10.1029/GM056p0021

Kronenberg, A. K., & Wolf, G. H. (1990). Fourier transform infrared spectroscopy determinations of intragranular water content in quartz-bearing rocks: Implications for hydrolytic weakening in the laboratory and within the earth. *Tectonophysics*, *172*, 255–271. https://doi.org/10.1016/0040-1951(90)90034-6

Kurt, H., Sorlien, C. C., Seeber, L., Steckler, M. S., Shillington, D. J., Cifci, G., . . . Carton, H. (2013). Steady late quaternary slip rate on the Cinarcik section of the North Anatolian fault near Istanbul, Turkey. *Geophysical Research Letters*, *40*, 4555–4559. https://doi.org/10.1002/grl.50882

Lasserre, C., Peltzer, G., Crampe, F., Klinger, Y., Van DerWoerd, J., & Tapponnier, P. (2005). Coseismic deformation of the 2001 $M_w = 7.8$ Kokoxili earthquake in Tibet, measured by SAR interferometry. *Journal of Geophysical Research*, *110*, B12408. https://doi.org/10.1029/2004JB003500

Leloup, P. H., Ricard, Y., Battaglia, J., & Lacassin, R. (1999). Shear heating in continental strike-slip shear zones: Model and field examples. *Geophysical Journal International*, *136*, 19040.

Luttrell, K., & Sandwell, D. (2010). Ocean loading effects on stress at near shore plate boundary fault systems. *Journal of Geophysical Research*, *115*, B08411. https://doi.org/10.1029/2009JB006541

Marco, S., Mordechai, S., & Agnon, A. (1996). Long-term earthquake clustering: A 50,000-year paleoseismic record in the Dead Sea graben. *Journal of Geophysical Research*, *101*, 6179–6191.

Mason, D. P. M., Little, T. A., & Van Dissen, R. J. (2004). *Influence of a fault-segment junction on the rupturing behaviour of the Awatere fault, New Zealand, and displacement-length measurement for the Marlborough earthquake rupture of 1848* (Res. Rep. 01/442, 148 pp.). Wellington, New Zealand: New Zealand Earthquake Commission.

Mason, D. P. M., Little, T. A., & Van Dissen, R. J. (2006). Rates of active faulting during late Quaternary fluvial terrace formation at Saxton River, Awatere fault, New Zealand. *Geological Society of America Bulletin*, *118*, 1431–1446. https://doi.org/10.1130/B25961.1

Matmon, A., Schwartz, D. P., Haeussler, P. J., Finkel, R., Lienkaemper, J. J., Stenner, H., & Dawson, T. E. (2006). Denali fault slip rates and Holocene–late Pleistocene kinematics of central Alaska. *Geology*, *34*, 645–648. https://doi.org/10.1130/G22361.1

McGill, S. F., Wells, S. G., Fortner, S. K., Kuzma, H. A., & McGill, J. D. (2009). Slip rate of the western Garlock fault, at Clark Wash, near Lone Tree Canyon, Mojave Desert, California. *Geological Society of America Bulletin*, *121* (3/4), 536–554. https://doi.org/10.1130/B26123

Meade, B. J. (2007). Power-law distribution of fault slip-rates in southern California. *Geophysical Research Letters*, *34*, L23307. https://doi.org/10.1029/2007GL031454

Meade, B. J., & Hager, B. H. (2004). Viscoelastic deformation for a clustered earthquake cycle. *Geophysical Research Letters*, *31*, L10610. https://doi.org/10.1029/2004GL019643

Meade, B. J., & Hager, B. H. (2005). Block models of crustal motion in southern California constrained by GPS measurements. *Journal of Geophysical Research*, *110*, B03403. https://doi.org/10.1029/2004JB003209

Meade, B. J., Hager, B. H., McClusky, S., Reilinger, R. E., Ergintav, S., Lenk, O., . . . Özener, H. (2002). Estimates of seismic potential in the Marmara Sea region from block models of secular deformation constrained by Global Positioning System measurements. *Bulletin of the Seismological Society of America*, *92*, 208–215. https://doi.org/10.1785/0120000837

Meade, B. J., Klinger, Y., & Hetland, E. (2013). Inference of multiple earthquake-cycle relaxation timescales from irregular geodetic sampling of interseismic deformation. *Bulletin of the Seismological Society of America*, *103*, 2824–2835. https://doi.org/10.1785/0120130006

Meade, B. J., & Loveless, J. P. (2009). Predicting the geodetic signature of $M_w \geq 8$ slow slip events. *Geophysical Research Letters*, *36*, L01306. https://doi.org/10.1029/2008GL036364

Meade, B. J., & Loveless, J. P. (2017). Block motion changes in Japan triggered by the 2011 great Tohoku earthquake. *Geochemistry, Geophysics, Geosystems*, *18*, 2459–2466. https://doi.org/10.1002/2017GC006983

Meghraoui, M., Aksoy, M. E., AkyüZ, H. S., Ferry, M., Dikbaş, A., & Altunel, E. (2012). Paleoseismology of the North Anatolian fault at Güzelkoy (Ganos segment, Turkey): Size and recurrence time of earthquake ruptures west of the Sea of Marmara. *Geochemistry, Geophysics, Geosystems*, *13*, Q04005. https://doi.org/10.1029/2011GC003960

Milliner, C. W. D., Dolan, J. F., Hollingsworth, J. C., Leprince, S., & Ayoub, F. (2016). Comparison of coseismic near-field and off-fault surface deformation patterns of the 1992 *Mw* 7.3 Landers and 1999 *Mw* 7.1 Hector Mine earthquakes: Implications for controls on the distribution of surface strain. *Geophysical Research Letters*, *43*, 10115–10124. https://doi.org/10.1002/2016GL069841

Nyst, M., & Thatcher, W. (2004). New constraints on the active tectonic deformation of the Aegean. *Journal of Geophysical Research*, *109*, B11406. https://doi.org/10.1029/2003JB002830

Oliot, E., Goncalves, P., & Marquer, D. (2010). Role of plagioclase and reaction softening in a metagranite shear zone at mid-crustal conditions (Gotthard Massif, Swiss Central Alps). *Journal of Metamorphic Geology*, *28*, 849–871. https://doi.org/10.1111/j.1525-1314.2010.00897.x

Oliot, E., Goncalves, P., Schulmann, K., Marquer, D., & Lexa, O. (2014). Mid-crustal shear zone formation in granitic rocks: Constraints from quantitative textural and crystallographic preferred orientations analyses. *Tectonophysics*, *612–613*, 63–80. https://doi.org/10.1016/j.tecto.2013.11.032

Oskin, M., & Iriondo, A. (2004). Large-magnitude transient strain accumulation on the Blackwater fault, Eastern California shear zone. *Geology*, *32*, 313–316.

Oskin, M., Perg, L., Shelef, E., Strane, M., Gurney, E., Singer, B., & Zhang, X. (2008). Elevated shear zone loading rate during an earthquake cluster in eastern California. *Geology*, *36*, 507–510. https://doi.org/10.1130/G24814A.1

Peltzer, G., Crampe, F., Hensley, S., & Rosen, P. (2001). Transient strain accumulation and fault interaction in the Eastern California shear zone. *Geology*, *29*, 975–978.

Pucci, S., D., Martini, P. M., & Pantosti, D. (2007). Preliminary slip rate estimates for the Düzce segment of the North Anatolian fault zone from offset geomorphic markers. *Geomorphology*, *97*, 538–554. https://doi.org/10.1016/j.geomorph.2007.09.002

Reilinger, R., Ergintav, S., Bürgmann, R., McClusky, S., Lenk, O., Barka, A., . . . Töksoz, M. N. (2000). Coseismic and postseismic fault slip for the 17 August 1999, M = 7.5, Izmit, Turkey earthquake. *Science*, *289*, 1519–1524. https://doi.org/10.1126/science.289.5484.1519

Reilinger, R., McClusky, S., Vernant, P., Lawrence, S., Ergintav, S., Cakmak, R., . . . Karam, G. (2006). GPS constraints on continental deformation in the Africa-Arabia-Eurasia continental collision zone and implications for the dynamics of plate interactions. *Journal of Geophysical Research*, *111*, BO5411. https://doi.org/10.1029/2005JB004051

Rockwell, T. K., Ragona, D., Seitz, G., Langridge, R., Aksoy, M. E., Ucarkus, G., . . . Akbalik, B. (2009). Palaeoseismology of the North Anatolian fault near the Marmara Sea: Implications for fault segmentation and seismic hazard, Palaeoseismology. In K. Reicherter, A. M. Michetti, & P. G. Silva (Eds.), *Historical and prehistorical records of earthquake ground effects for seismic hazard assessment: The Geological Society, London, special publications* (Vol. 316, pp. 31–54). London, UK: Geological Society. https://doi.org/10.1144/SP316.3

Romanowicz, B. (1993). Spatiotemporal patterns of energy release in great earthquakes. *Science*, *260*, 1923–1926.

Sammis, C. G., Smith, J. C., Schubert, G., & Yuen, D. A. (1977). Viscosity-depth profile of the Earth's mantle: Effects of polymorphic phase transitions. *Journal of Geophysical Research*, *82*, 3747–3761.

Savage, J. C. (2000). Visco-elastic coupling model for the earthquake cycle driven from below. *Journal of Geophysical Research*, *105*, 25,525–25,532.

Savage, J. C., & Burford, R. O. (1973). Geodetic determination of relative plate motion in central California. *Journal of Geophysical Research*, *78*, 832–845.

Savage, J. C., & Prescott, W. H. (1978). Asthenosphere readjustment and the earthquake cycle. *Journal of Geophysical Research*, *78*, 3369–3376.

Schwartz, D. P., Haeussler, P. J., Seitz, G. G., & Dawson, T. E. (2012). Why the 2002 Denali fault rupture propagated onto the Totschunda fault: Implications for fault branching and seismic hazards. *Journal of Geophysical Research*, *117*, B11304. https://doi.org/10.1029/2011JB008918

Sella, G. F., Dixon, T. H., & Mao, A. (2002). REVEL: A model for recent plate velocities from space geodesy. *Journal of Geophysical Research*, *107*(B4), https://doi.org/10.1029/2000JB000033

Takeuchi, C. S., & Fialko, Y. (2012). Dynamic models of interseismic deformation and stress transfer from plate motion to continental transform faults. *Journal of Geophysical Research*, *117*, B05403. https://doi.org/10.1029/2011JB009056

Thatcher, W. (2009). How the continents deform: The evidence from tectonic geodesy. *Annual Review of Earth and Planetary Sciences*, *37*, 237–262.

Thatcher, W., & England, P. C. (1998). Ductile shear zones beneath strike-slip faults: Implications for the thermomechanics of the San Andreas fault zone. *Journal of Geophysical Research*, *103*, 891–905.

Van der Woerd, J., Mériaux, A.-S., Klinger, Y., Ryerson, F. J., Gaudemer, Y., & Tapponnier, P. (2002a). The 14 November 2001, Mw = 7.8 Kokoxili earthquake in Northern Tibet (Qinghai Province, China). *Seismological Research Letters*, *73*, 125–135. https://doi.org/10.1785/gssrl.73.2.125

Van der Woerd, J., Tapponnier, P., Ryerson, F. J., Mériaux, A.-S., Meyer, B., Gaudemer, Y., . . . Zhiqin, X. (2002b). Uniform postglacial slip-rate along the central 600 km of the Kunlun fault (Tibet), from ^{26}Al, ^{10}Be, and ^{14}C dating of riser offsets, and climatic origin of the regional morphology. *Geophysical Journal International*, *148*, 356–388. https://doi.org/10.1046/j.1365-246x.2002.01556.x

Weldon, R., Scharer, K., Fumal, T., & Biasi, G. (2004). Wrightwood and the earthquake cycle: What a long recurrence record tells us about how faults work. *GSA Today*, *14*(9), 4–10.

Xu, X., Chen, W., Ma, W., Yu, G., & Chen, G. (2002). Surface rupture of the Kunlunshan earthquake (Ms 8.1), northern Tibetan plateau, China. *Seismological Research Letters*, *73*(6), 884–892.

Yanchilina, A. G., Ryan, W. B. F., McManus, J. F., Dimitrov, P., Dimitrov, D., Slavova, K., & Filipova-Marinova, M. (2017). Compilation of geophysical, geochronological, and geochemical evidence indicates a rapid Mediterranean-derived submergence of the Black Sea's shelf and subsequent substantial salinification in the early Holocene. *Marine Geology*, *383*, 14–34. https://doi.org/10.1016/j.margeo.2016.11.001

Zinke, R., Dolan, J. F., Rhodes, E. J., Van Dissen, R., & McGuire, C. P. (2017). Highly variable latest Pleistocene1 Holocene incremental slip rates on the Awatere fault at Saxton River, South Island, New Zealand, revealed by lidar mapping and luminescence dating. *Geophysical Research Letters*, 44. https://doi.org/10.1002/2017GL075048